

A NUMERICAL STUDY ON THE BEHAVIOR OF STONE COLUMNS WITH DIFFERENT AREA RATIOS IN SOFT CLAYS

Husam Hikmat Baqir¹, Mohammed Faeq Aswad¹ and *Mohammed Yousif Fattah¹

¹Civil Engineering Department, University of Technology, Baghdad, Iraq.

*Corresponding Author, Received: 12 Dec. 2023, Revised: 04 March 2023, Accepted: 5 March 2024

ABSTRACT: The single floating stone column behavior in very soft soils with a low undrained shear strength of $C_u \leq 20$ kN/m² was studied in the finite-element method to investigate the influence of stone column's area ratio on the normalized pressure-settlement curves of circular footings of different diameters. The studied cases consist of stone columns of 1.0 m in diameter D_s and lengths L_s of (4 m, 6 m, and 7.5 m). The diameter of footings D_f is (1.0 m, 1.2 m, 1.4 m, 1.6 m, 2.0 m, 2.5 m, and 3.5 m) which covers the area ratios with a range of 100 to 8.16 %. A total of 28 runs were carried out using the Ansys program to simulate the case for improved and unimproved soil. In the axisymmetric numerical model, the connection between the stone column and the adjacent contact clay soil was modeled as bonded type. The results of the analysis showed that there is a clear relationship between the bearing ratio $(q/cu_{improved}) / (q/cu_{unimproved})$ and the normalized settlement (S/D_f) of the composite structure and the area ratio $Ar\%$ of the stone columns. The deformation ratio $(S_{treated}/S_{untreated})$ and the footing diameter are related using a straightforward equation. In comparison to footings with a low area ratio, the footing displays a lower value of settling when subjected to the same pressure. By decreasing the diameter of the footing, the normalized settlement decreases for the same normalized q/cu values. The bearing ratio depends on the stone column length ratio L_s/D_s and settlement ratio. It is from 2.2 at a 100% area ratio and 1.23 at a 16% area ratio.

Keywords: Stone column, Area ratio, Finite elements, Bearing ratio, Lateral deformation.

1. INTRODUCTION

Soft soils are found in the world in many places, these types of soils are characterized by their low shear strength, which is typically less than 25 kN/m², with a high compressibility that leads to many foundation problems. A variety of approaches have been used to improve the mechanical properties of these soils. The stone column is often one of the low-cost techniques in comparison to other techniques used to enhance the load-bearing capacity and reduce the final settlement and the settlement duration, especially for large areas and under embankments Hughes and Withers [1].

Embankments and natural slopes are successfully improved in performance by using the stone column's technique which enhances the shear strength and reduces the settlement and time required for settlement to be accomplished. In addition, the low cost of this technique is superior due to the low cost of execution and environmental benefit making this technique among other types of soil improvement. Stone columns are ordinarily used for the improvement of soft soils. For the different structures' support, the stone columns have been increasingly used recently. Stone columns are used to reduce settlement and increase the carrying capacity of soft soils at a cost that is both economical and environmentally beneficial Hughes et al. [2].

Hughes and Withers [1] and Hughes et al. [2], recently investigated the stone column bulging failure, using a model and field measurement. They found

that after the critical length (a four-stone column's diameter) is exceeded, bulging failure is the most common type of stone column failure.

One of the most common techniques for improving soft soils for the foundation of embankments or structures is stone columns, also known as granular piles or aggregate piers. Ground improvement by a stone column was believed to be a cost-effective method, as stated in [3-5]. Stone column involves improving weak soils by installing vertical boreholes in the ground, filled upwards with aggregates, and compacted by a vibrator. Stone columns have been widely applied when dealing with soft soil to enhance its bearing capacity, decrease settlements, improve the stability of slopes [6, 7], reduce the liquefaction under cyclic loads [8], and accelerate consolidation times [9]. There are two types of stone columns; end-bearing and floating stone columns. The end-bearing stone column is a term indicated when the toe of the stone column was placed on the hard stratum. While for The floating stone columns, also known as partially penetrated stone columns, are assumed to partially penetrate the soft soil as the hard strata are far underneath the surface [10-12].

The ratio of the stone column area to the total area is a concept known as the area ratio ($Ar\%$) for the unit cell idea, however, it will be the area of the stone column divided by the footing area for a single stone column.

The spacing between stone columns is a significant factor in determining the group's bearing

capability. Rao and Madhira [13] noticed that by increasing the stone column spacing above a certain value, there was a reduction in its bearing capacity.

Fattah and Majeed [14] used the finite elements method to simulate the encasing of stone columns by geogrid material to increase its performance in different conditions. They used CRISPR-2D for the analysis of the composite system. The elastic completely plastic model was used by the Mohr-Coulomb failure criterion. The parametric study was to investigate the effect of encasing and the length of stone columns. It was found that the length-to-diameter ratio L_s/D_s of (7-8) for the standard technique produces the maximum performance when the shear strength ranges between (20-40) kPa, but when the shear strength decreases to 10 kPa, the L_s/D_s ratio was (10-11) while the best performance for encased techniques was when the length to diameter ratio L_s/D_s between (7-8). The bearing ratio for the encased floating columns improves as the area ratio increases, especially when the ratio reaches (0.25). In comparison to typical stone columns, the geogrid lowers the lateral movement.

Nasab and Asakereh [15] presented the results of a series of finite element calculations on square footing resting on both improved and unimproved soil. One of the existing experimental reports was used to validate the generated model. The parametric studies were then carried out to identify the effective geometrical and mechanical parameters, as well as their influence on footing bearing capacity. The use of stone columns boosted the footing bearing capacity significantly, according to the findings. The bearing capacity ratio (BCR) increases as the stone column friction angle increases and the cohesion and friction angle of the soft soil decrease.

Fattah et al. [16] studied the behavior of embankment models that were supported by ordinary and encased stone columns (ESCs). Different spacing distances were used in the model tests., length to diameter ratios (L_s/D_s), as well as different heights of the embankment. A total number of 39 model tests were carried out on soil having 10 kPa of undrained shear strength. They revealed that for embankment models the encasement of stone columns ESCs provides the most efficient way for bearing improvement regardless of the stone columns being floated or rested on a rigid stratum. The bearing ratio for the encased technique in comparison to untreated soil was 1.4, 1.57, and 1.83 in comparison with ordinary type which gives the ratio of 1.29, 1.39, and 1.63 respectively for embankment heights of (200, 250, 300 mm) with ($L=d=5$ and 8), and spacing ($s=2.5d$). The settlement for these cases was reduced by approximately 0.63, 0.6, and 0.45 times that of untreated and 0.71, 0.67, and 0.62, respectively.

Garakani et al. [17] used the concept of suction-dependent effective stress for the determination of the bearing capacity of shallow footing lying on

unsaturated soils, two approaches were used, the first is a new analytical solution. They extended Vesic's solution for saturated soils and they proposed a modification factor for tuning the cohesion-dependent component in the bearing capacity equation.

Experimental research on the impact of construction methods on the functionality of stone columns was done by Nazariafshar et al. [18]. Stone column models with diameters of (6 and 8 cm), which are a floating type, are both uncased and covered with geotextile and were built using displacement and replacement methods. It was demonstrated that stone columns built using the displacement method have a bearing capacity that is 20–30% greater than stone columns constructed by the replacement method, and the impacts of the construction method on the bearing capacity are more apparent in stone columns with larger area replacement ratios. By adjusting the stress concentration ratio (n) and load improvement ratio (LIR), the performance of stone columns was also examined. It was demonstrated that the area replacement ratio and length-to-depth ratio have an impact on both LIR and n . When the settlement ratio reaches 5% or greater, LIR and n begin to approach a constant value. To assess the stiffness and bearing capacity of stone columns, a design curve is ultimately produced.

Shreya and Peter [19] represented the loose to dense condition of the granular material of the stone column in their study using soft clay with a stiffness of 15 MPa and varied the stiffness of the stone column (E_{gp}) in the range of 75 to 190 MPa with a relative stiffness (E_{gp}/E_s) varying between 5 and 13. They also varied the size of the stone column as represented by the area ratio (A_r), which ranged from 0.07 to 0. The investigation demonstrated that regardless of the area ratio and total stress (q_{total}), Q_{gp}/Q_s change concerning E_{gp}/E_s is logarithmic. For q_{total} 15 t/m² for all area ratios, this Q_{gp}/Q_s fluctuation with E_{gp}/E_s is relatively minor, but for larger q_{total} values, considerable variance is seen for smaller A_r , which reduces with the rise in A_r .

As a method for enhancing strength in loose soils, Gharavi et al. [20] examined the load-carrying capacity response of gravel-shredded tire stone column groups. Large-scale oedometer studies on groups of gravel and gravel-shredded tire mixtures with varying tire composition, arrays, and spacings were used in the experimental study. The findings showed that adding more tires can have a negative impact on the load-settlement behavior of the stone column groups in combinations comprising 20% of the shredded tire. Additionally, adding an ideal tire to the stone column components increases the bed soil's stiffness (Young's modulus). This behavior is closely tied to the area ratio and friction angle caused by various configurations of the stone column groups.

The purpose of this study is to determine the

impact of the area ratio A_r on the bearing and settlement characteristics of the composite structure of floated stone column to ensure choosing the appropriate footing diameter that gives the optimal performance for the soil, stone column, and footing system and suggest correlations between many parameters to predict the settlement and the bearing capacity through finite element analysis. It is known that increasing the area ratio of stone columns results in more improvement in the soil behavior, but details of this improvement depend on several parameters that will be investigated in this study.

2. ANSYS PROGRAM VERIFICATION

The ANSYS 18 Workbench output results were validated by comparing them to the findings of an experimental load-settlement test performed by Fattah et al. [21] using a finite element model of a single-floated axisymmetric stone column. A single floating stone column with dimensions of 50 mm in diameter by 400 mm in length was used as the experimental model. It was put in the center of an 800-mm-high clay bed inside a steel tank that measured 1100 mm by 1000 mm by 800 mm in size. A sturdy steel plate with a 50 mm diameter was used to gradually apply the load. The characteristics of soft clay materials and stone columns are displayed in Table 1.

Fig. 1 illustrates the finite element results as well as the validation of the experimental work by Fattah et al. The quality of the model used in this work is demonstrated by the good agreement between ANSYS 18 finite element results and the experiment's results performed by Fattah et al. [21].

Table 1 List the physical characteristics of the soft clay and stone materials used in Fattah et al.'s experiments [21].

Material	Clay	Stone column
Modulus of elasticity (kN/m ²)	6000	45000
Poisson's ratio	0.45	0.3
Cohesion (kN/m ²)	12	0
Angle of internal friction (Deg.)	0	38

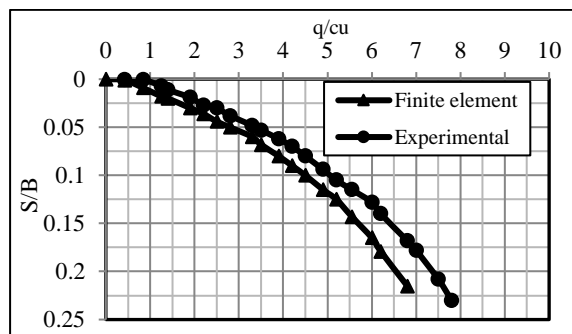


Fig.1 Comparison of results obtained by Fattah et al. [11] experimental work and ANSYS 18 Workbench.

3. PROBLEM DESCRIPTION

The case study consists of a circular footing laying on both clay and stone columns. The analysis of the case was performed by utilizing software called Workbench 18.0 ANSYS. The case study comprises a circular single concrete footing of 500 mm thickness and with many diameters which are (0.8, 0.9, 1.0, 1.2, 1.4, 1.6, 2.0, 2.5, and 3.0) m. The footing is supported by a single floating stone column with different diameters (0.8, 1.0 m) and different lengths (4, 6, 7.5). The used lengths are equal to or more than the critical length which is equal to (4D_s) as recommended by Hughes and Withers [1] to ensure a bulging failure type that occurs in the stone column. The length-to-diameter ratio was selected based on previous studies such as Fattah et al. (2013) and Fahmi et al. (2019) [22-23]. The distance of the boundary of the surrounding clay was 4.0 m in radius from the Y-axis of the symmetry line, and a depth of 12 m, as illustrated in Fig. 2, which demonstrated the half structure case to use the analysis of 2D axisymmetry to minimize time and data amount required if using 3D analysis to solve the problem. The properties of the soft clay were 20 kN/m² undrained shear strength and 0.49 Poisson's ratio with an assumed modulus of elasticity to be equal to 500 times the shear strength of the soft clay based on empirical correlations as suggested by Bowles [24]. The physical characteristics of the clay used in the study and the backfill material utilized in stone columns are listed in Table 2.

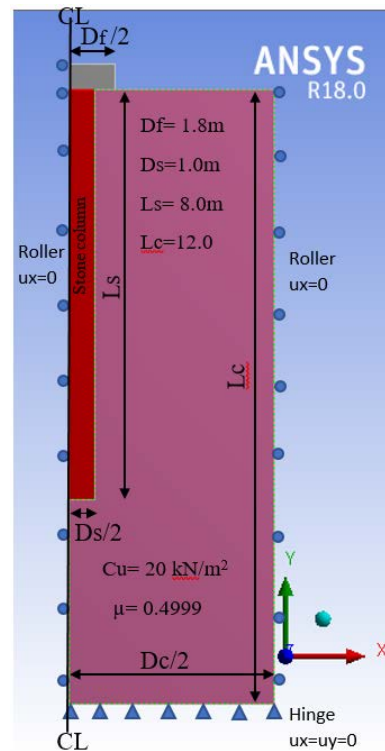


Fig.2 Problem schematic diagram.

Table 2 The used clay and stone column properties.

Specification	Material	
	Clay	Stone column
Unit weight, (kN/m ³)	19	21
Young's modulus, (kN/m ²)	1×10 ⁴	1×10 ⁵
Poisson's Ratio	0.499	0.35
Cohesion, (kN/m ²)	20	0
Internal friction angle, (Degree)	0	45
Dilatancy angle, (Degree)	0	15
Residual cohesion, (kN/m ²)	20	0
Residual friction angle, (Degree)	0	30

3.1 Program Data

The structure is constructed by using the ANSYS claim and then exported to the program to apply the material properties for each of the stone, clay, and concrete. After that, the contact element is specified for all contact materials. In this analysis, an axisymmetric (PLANE183) element was used, with (Ux and Uy) degree of freedom. The element was restricted by the bottom and right boundaries, the size of the element was fixed to a length of 100 mm, to divide the problem into uniform elements and to improve output accuracy. A surface-to-surface contact element (CONTA172) and (TARGE169) are used to mimic the interaction between the surrounding clay, stone columns, and footing. This type of element was selected as bonded since the stone will pierce the clay layer. The finite element mesh for the composite structure is shown in Fig.3.

The number of points between these limitations was selected so that each element would have a length of 10 mm in order to compare the induced stresses and deformations for different footing diameters for points located in the same location. For example, for a footing with a radius of, a construction geometry path was inserted between two points starting from the symmetry line of the bottom of the footing and the edge of the footing. The total points number is 59, resulting in 60 sublines with a length of 10 mm apiece. The boundaries of the composite (foundation, stone columns, and clay) were represented by horizontal displacements equal to zero ($U_x = 0$) and in the y- direction, free displacements except for the bottom of the composite (the last layer of clay), zero horizontal and vertical displacement were considered ($U_x = U_y = 0$).

For all load instances, a single ramping step of stress equal to 1.0 kN/m² was applied equilly and gradually in the Y-direction to the top surface of the footing until the load achieved the desired total load or obtained a high deformation value. During the solution phase, the auto time stepping was disabled to force the software to follow this approach without automatically adjusting the load, for example, the

sub-steps for a total stress of 600 kN/m² will be 600 steps. This process will help in a better comparison between the different loading cases in terms of pressure.

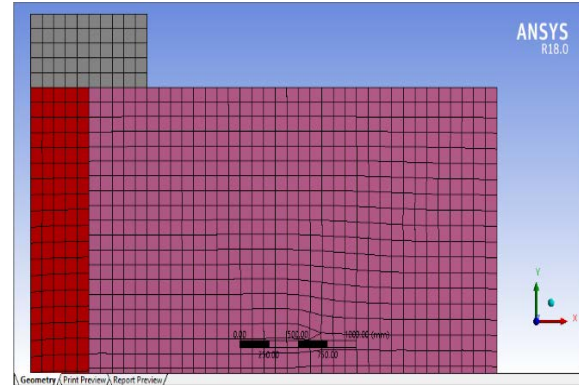


Fig.3 Finite elements mesh illustrate the composite of stone columns and concrete footing and the clay soil, $D_f = 2$ m and $D_s = 1.0$ m.

4. RESULTS AND DISCUSSION

The solving process starts after the insertion of all the needed data, where the loads increase gradually in steps until reaching a specified stress or deformation and then the results are presented by the load settlement at specified points, for the comparison between the studied cases.

The results are presented in dimensionless form, where the applied vertical stresses are divided by the undrained shear strength of the soft clay (q/c_u) and the corresponding settlements are divided by the footing's diameter (S/D_f). In addition, the dimensionless ratio of stresses of the treated soil to that of the untreated soil is defined and denoted by bearing ratio = $((q/c_u) \text{ treated soil}) / ((q/c_u) \text{ untreated soil})$ and again the dimensionless ratio of settlement of the treated and untreated soil will be denoted by the term deformation ratio = $[(S/D_f) \text{ treated soil}] / [(S/D_f) \text{ untreated soil}]$. These definitions will be very useful for comparison between the results of the different types of footing.

Fig. 4 shows the results of pressure-settlement curves for unimproved case and improved case with a diameter 1 m and length 7.5 m of stone column, which presents L_s/D_s of 7.5 at different area ratios ($A_r\%$), where ($A_r\%$ is the area of stone column devited by the area of footing). For clarification, the unimproved load-settlement curve consists of seven curves that represent the different diameters of a single footing resting on the surface of the composite structure but when they are normalized by dividing the pressure by c_u and the settlement by D_f , they all are transformed into one coinciding curve. Similar curves are obtained for stone columns of diameters 0.8 and 1 m having L_s/D_s of 4 and 6.

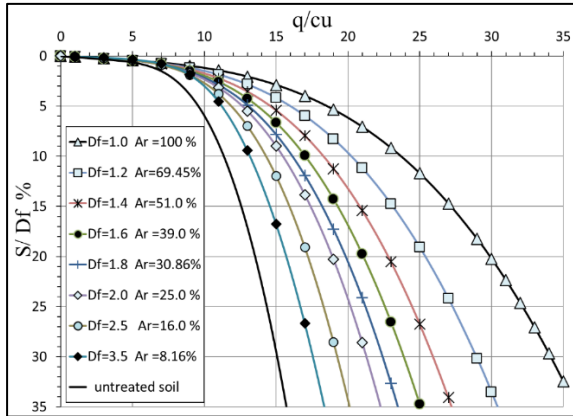


Fig.4 Normalized curves for pressure-settlement relationship for different area ratios Ar %, (Ls / Ds = 7.5).

From Fig. 4, the area ratio Ar % shows a clear effect on the normalized pressure-settlement relationship of a footing resting on a single floating stone column. Under the same pressure, the footing exhibits a lower value of settlement in comparison with footings having low area ratios. The normalized settlement diminishes with lowering the diameter of the footing under the same normalized q/cu values. On the other hand, as the diameter of the footing decreases, the normalized q/cu rises for the same normalized s/Df values. This is due to the fact that, for the same stresses applied to the footing, as the diameter of the stone column (Ds) is quantified and the diameter of the footing is increased, the corresponding area ratio decreases. This causes increased stress to be transmitted to the clay area and increased deformation of the composite structure.

Fig. 5 shows the result of the total deformation in mm, in the composite structures for the case when Ls/Ds = 7.5 the stone diameter is 1 m and has a length of 7.5 m when the applied pressure is 200 kN/m² at the top of 1.6 m circular footing which is corresponding to 39% area ratio. The figure shows that the deformation is concentrated around the stone column area and decreases with depth until reaching a zero amount on both the stone and clay layers. The shape of the total deformation is similar to the bulging shape expected for this type of foundation. A similar behavior is shown in Fig. 6 which relates the vertical deformation for the same loading conditions and footing's dimensions again, the bulging shape is observed around the stone column.

Fig. 7 depicts the relationship between the "bearing ratio" and the area ratio Ar percent for varied Ls/Ds of (4, 6, and 7.5) and varying S/Df percentages of 5% to 25%. All curves within the studied cases show a similar linear trend that with the increase in area ratio, the amount of bearing ratio also increases, and for different length-to-diameter ratios, the relationship is in correspondent. For a specified area ratio, the gain in the bearing ratio is marginal when

the S/Df exceeds 15% in all Ls/Ds values.

The bearing ratio for Ls/Ds = 7.5 and S/Df = 20% ranges from (2.2 at 100% area ratio to 1.265 at 16% area ratio), while the bearing ratio for Ls/Ds = 6 and S/Df is 20% ranges from (2.2 at 100% area ratio to 1.268 at 16% area ratio) and finally the bearing ratio for Ls/Ds = 4 and S/Df is 20% is ranging from (2.2 at 100% area ratio to 1.23 at 16% area ratio). All these numbers are coinciding despite the fact that they have different Ls/Ds values which indicate that the stone column length did not affect the bearing ratio.

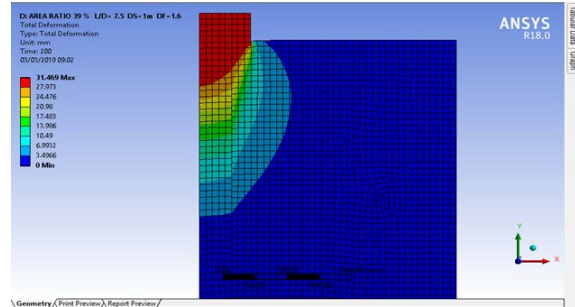


Fig.5 Total deformation for an applied pressure of 200 kN/m² (max. Y-displacement = 31.469 mm).

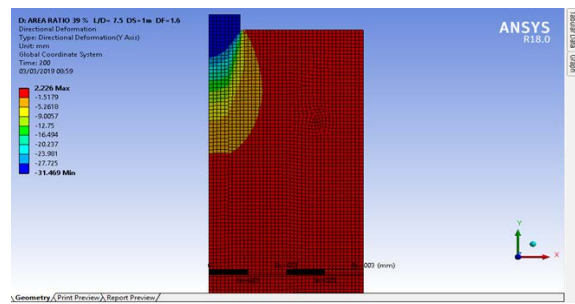


Fig.6 Deformation in the Y-axis of the footing-stone column system under applied pressure of 200 kN/m², (max. Y-displacement =31.469 mm).

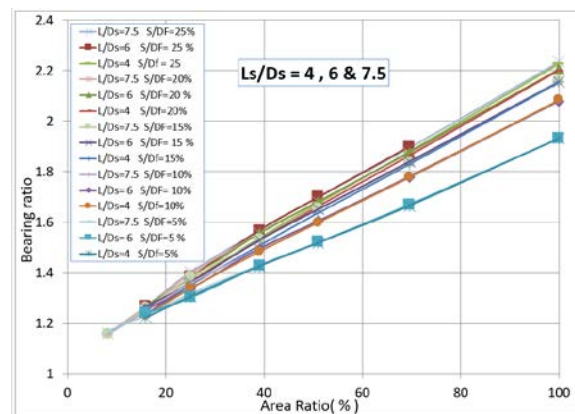


Fig.7 Area ratio Ar % vs. bearing ratio relationship.

The bearing ratio for Ls/Ds = 7.5 and S/Df = 5% ranges from (1.93 at 100% area ratio to 1.23 at 16% area ratio) while the bearing ratio for Ls/Ds = 6 and S/Df is 5% ranges from (1.93 at 100% area ratio to 1.24 at 16% area ratio) and finally the bearing ratio

for $L_s/D_s = 4$ and S/D_f is 5% is ranging from (1.93 at 100% area ratio to 1.22 at 16% area ratio). Again, the effect of the length is marginal and with increasing the area ratio, the difference in bearing pressure lines of the 20% and 5% S/D_f also increased. The variation of bearing ratio with S/D_f for different area ratios is presented in Fig. 8. When the soil is enhanced by shorter stone columns, the increase in the replacement area ratio results in a major rise in the bearing capacity. Simultaneously, as the replacement area ratio increases, the settlement reduction of the loaded area increases.

The findings of Sarmurat et al. [25] that indicated the preventative impact of using stone columns are consistent with the results. They demonstrated that this beneficial effect was more pronounced when the area ratio and relative density were raised. The application of stone columns improves soil when suitable designs are created in accordance with the characteristics of the soil.

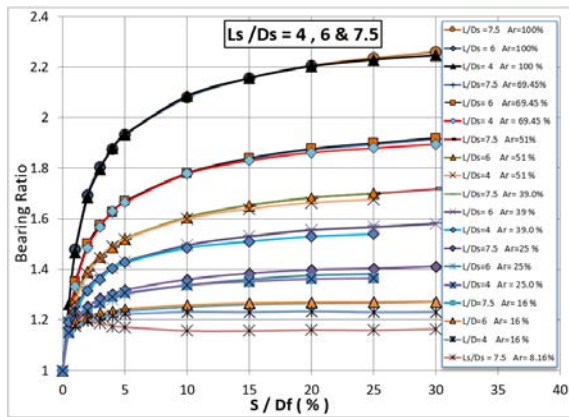


Fig.8 Variation of bearing ratio with the settlement ratio S/D_f for different cases.

Fig. 8 clarifies that the bearing ratio increases rapidly with the increase of the normalized settlement until reaching S/D_f of 5%, for an area ratio less than 39%, after which the slope of the curve decreases to a steady value but for an area ratio higher than 40%, the steady value is achieved after passing S/D_f of 15% and for area ratio of 100%, the steady value is reached after passing S/D_f of 20%. Fig. 9 shows the relation between the deformation ratio and the normalized pressure (q/cu) applied on the circular footing for different area ratios. It is interesting that all the curves show a similar trend in which the settlement improvement decreases at low stresses up to a value of $(q/cu) = 2$, after this stress, the curves reach a flattened zone until reaching a stress of $(q/cu) = 4$. Beyond this value, the deformation ratio increases with the increase of stress till reaching a semi-constant value approximately at $(q/cu) = 15$.

The highest improvement was obtained for footings of low area ratio, thus the increase in the area ratio will result in a deformation ratio which is observed for the footing of a larger area ratio in

comparison to the highest improvement in settlement.

Fig. 10 presents the reformatting of the previous data but for $L_s/D_s = 7.5$ case only, the vertical axis is the inverse of the deformation ratio plotted against the (q/cu) . The resulting figure shows that the improvement ratio is higher when (q/cu) exceeds 8 in comparison with low values of stresses. A similar behavior is observed for the other L_s/D_s ratios.

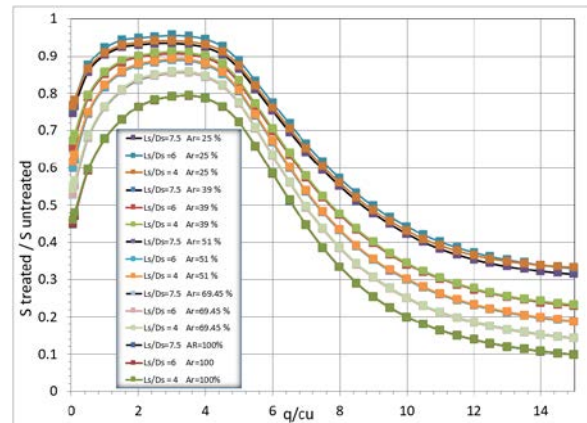


Fig.9 Deformation ratio vs. normalized pressure for different area ratios.

The interaction between the stone column material and the surrounding soil determines the load transfer between the stone column and the surrounding soil. When the surrounding soil is soft, this interaction is quite weak. The surrounding soil shear strength determines the skin friction along the columns; as it grows with an increase in the weight supported by the column. This may not be the case if the shear strength is larger than 12 kPa, in which case the interaction becomes apparent.

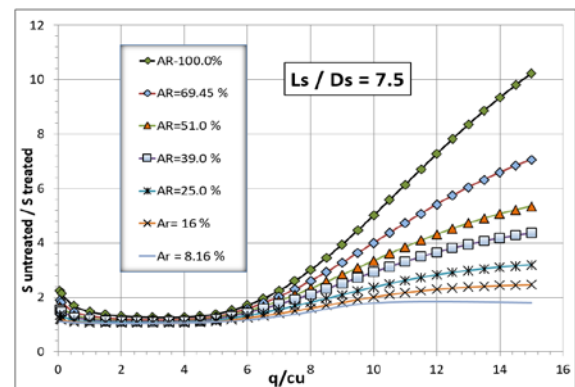


Fig.10 Normalized pressure vs. normalized settlement for L_s over $D_s=7.5$.

Figs. 11, 12, and 13 show the relation between the deformation ratio divided by the footing's diameter for each case and the normalized stresses (q/cu) for L_s/D_s of 7.5, 6, and 4, respectively. It is interesting that all the curves show a similar behavior to Figure 8 but in a reverse manner; the curves are no longer parallel but they are overlapped and intersect at nearly

a certain point when $(q/cu) = 9$ and corresponding $St/Sun/Df$ of about 0.25. This is true for the majority of area ratios encountered in the engineering field. The exact behavior is observed for $(Ls/Ds) = 6$ and 4, for all area ratios higher than 25%, all the curves are intersecting at the same point when (q/cu) is 9 and $((St/Sun)/Df)$ is 0.25.

The present results are consistent with those of Fattah and Majeed [26] who found that the strength of the column increases with the increase in the length of the stone column. The effective length-to-diameter ratio of the stone column is found to be $L/d = (7-8)$ for all area ratios and after L/d of 8, there is no effect on the $(q \text{ treated}/q \text{ untreated})$ value.

The outcomes are consistent with those of Naik [27], who discovered that, for a given length of stone column, the primary stress is greatest at the upper area ratio and that it rises linearly as the length ratio rises. Additionally, the maximum area-to-length ratio and the maximum failure stress are related. The failure zone rises to the upper side of the pond ash bed after attaining the maximum failure stress.

Fattah et al. [28] concluded that the performance of stone column embankments relies upon the ability of the granular embankment material to arch over the “gaps” between the stone columns’ spacing. This is due to reduced stress concentration on columns by soil arching and more punching of stone columns.

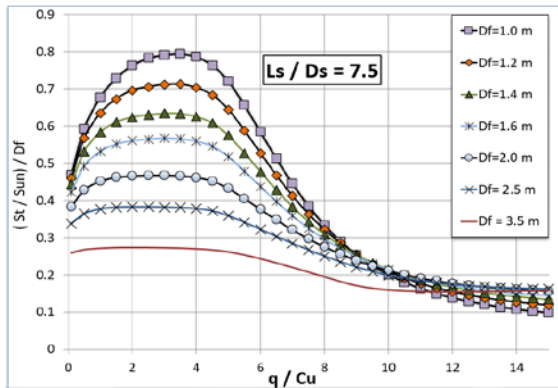


Fig.11 Deformation ratio / Df vs. normalized pressure for Ls over Ds =7.5.

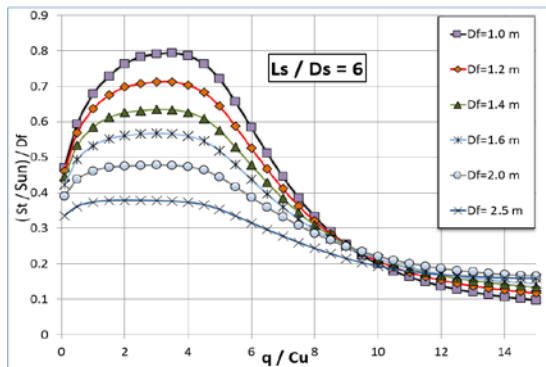


Fig.12 Deformation ratio / Df vs. normalized pressure for Ls/Ds =6.

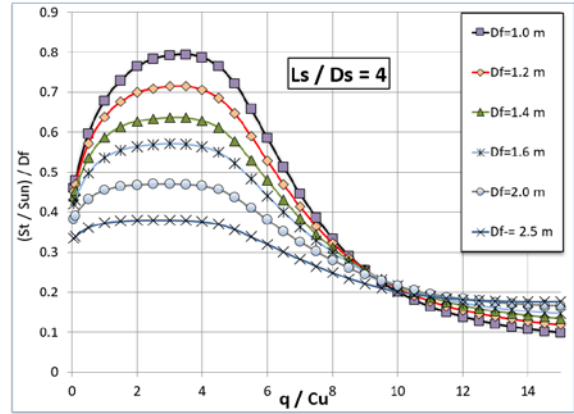


Fig.13 Deformation ratio over Df vs. normalized pressure for Ls/Ds =4.

There is an interesting correlation that relates the applied pressure with the settlement of the improved and unimproved soil in addition to the undrained shear strength of the clay layer and finally the diameter of the footing. This correlation is described below:

$$\left(\frac{S_{\text{treated}}}{S_{\text{untreated}} \times Df} \right) = 0.25 \quad (1)$$

when $(q/cu) = 9$
or can be written in the form:

$$\left(\frac{S_{\text{treated}}}{S_{\text{untreated}}} \right) = \frac{Df}{4} \quad (2)$$

when $(q/cu) = 9$ and area ratio $(Ar\%) \geq 25\%$.

If the failure is assumed to occur at stress $(q = 9 * cu)$, then the settlement of the treated composite structure can be estimated by knowing the settlement of the untreated soil for the same footing diameter or choosing the appropriate diameter for the footing by fixing the percent of settlement of treated to untreated soil.

“However, close to the stone column, the strains in soil may be large, particularly in soft clays, hence other numerical methods may be more suitable for this problem.” (Shafee and Khoshghalb, 2022)[29].

5. CONCLUSIONS

The present study includes a finite element analysis of a floating stone column in soft clay soil. So, the results obtained are limited to the condition analyzed. The following conclusions could be obtained:

1. There is a clear effect of the area ratio on the normalized load-settlement curves of a footing resting on a single floating stone column. Under the same pressure, the footing exhibits a lower value of

settlement in comparison with footings having a low area ratio. Under the same stress level, the footing with the larger area ratio exhibits minimal lateral deformation.

2. The normalized settlement declines as the diameter of the footing is reduced under the same normalized q/cu values. There were decreases in settlement improvement at low stresses up to a value of $(q/cu) = 2$. After this stress, the curves reach a flattened zone until reaching a stress of $(q/cu) = 4$. Beyond this value, the deformation ratio increases with the increase of stress till reaching a semi-constant value approximately at $(q/cu) = 15$.

3. The bearing ratio depends on the stone column length ratio L_s/D_s and settlement ratio. It is from 2.2 at a 100% area ratio and 1.23 at a 16% area ratio.

4. The deformation is concentrated around the stone column area and decreases with depth until reaching a zero amount on both the stone and clay layers. The shape of the total deformation is similar to the bulging shape expected for this type of foundation.

5. A correlation is derived which relates the settlement of the improved and unimproved soil in addition to the undrained shear strength of the clay layer and finally the diameter of footing.

6. REFERENCES

- [1] Hugher, J. M. O. and Withers, N. J., Reinforcing of soft cohesive soils with stone columns, *Gr. Eng.*, Vol. 7, No. 3. (1974), pp.42-49.
- [2] Hughes, J. M. O., Withers, N. J., and Greenwood, D. A., A Field Trial of the Reinforcing Effect of a Stone Column in Soil, *Geotechnique*, Vol. 25, No. 1, 1975, pp. 31–44.
- [3] Van Impe W., and De Beer, E., Improvement of settlement behavior of soft layers by means of stone columns, 8th European Conference on Soil Mechanics and Foundation Engineering, Helsinki 1, 1983, pp. 309–312.
- [4] Stuedlein, A., and Holtz, R., Displacement of spread footings on aggregate pier reinforced clay, *Journal of Geotechnical and Geoenvironmental Engineering*, vol.140, No.1, 2014, pp. 36–45.
- [5] Vahedian, A., Mahini, S., and Aghdaei, S., A short state of the art review on construction and settlement of soft clay soil reinforced with stone column, *Int. J. Eng. Tech.*, vol. 6, No.5, 2014, pp. 420-425.
- [6] Vautrain, J., Reinforced earth wall on stone columns in soil, *Proc. Int. Symp. on Soft Clay*, Asian Inst. Technol., Bangkok, 1977, pp.613-626.
- [7] Barksdale, R. and Bachus, R., Design and construction of stone columns, Rep. No. FHWA/RD 83/026, Federal Highway Administration, Washington, DC (1983).
- [8] Stuedlein, A., Abdollahi, A., Mason, H., and French, R., Shear wave velocity measurements of stone column improved ground and effect on site response, *International Foundation and Equipment Expo*, 2015, pp. 2306- 2317.
- [9] Han, J., and Ye, S.L., A simplified solution for the consolidation rate of stone column reinforced foundations., *Journal of Geotechnical and Geoenvironmental Engineering*, 127(7), 2001, pp. 597–603.
- [10] Ng KS, Tan SA, Design and analyses of floating stone columns, *Soils Found*, 54(3), 2014, pp. 478–487 (2014).
- [11] Bong, T., Stuedlein, A. W., Martin, J., and Kim, B, Bearing capacity of spread footings on aggregate pier–reinforced clay: updates and stress concentration. *Canadian Geotechnical Journal*, 57(5), 2020, pp. 717-727.
- [12] Stuedlein, A. W., and Holtz, R. D., Analysis of footing load tests on aggregate pier reinforced clay. *Journal of Geotechnical and Geoenvironmental Engineering*, ASCE, 138(9), 2012, pp. 1091-1103.
- [13] Rao, L. and Madhira, M., Evaluation of Optimum Spacing of Stone Columns, in *Geotrendz Proceedings of the Indian Geotechnical Conference.*, 2010.
- [14] Fattah, M. Y. and Majeed, Q. G., A study on the behaviour of geogrid encased capped stone columns by the finite element method, *Int. J. GEOMATE*, Vol. 3, No. 1, 2012, pp. 343–350.
- [15] Nasab M. Jaber, Numerical Analysis of the Bearing Capacity of Stone Columns Improved Ground., *Int. J. Integr. Sci. Innov. Technol.* 4, 2015, pp. 1–5.
- [16] Fattah, M. Y., Zabar, B. S. and Hassan, H. A., Experimental analysis of embankment on ordinary and encased stone columns, *Int. J. Geomech.*, Vol. 16, No. 4, 2016, pp. 507-534.
- [17] Akbari Garakani, A., Sadeghi, H., Saheb, S. and Lamei, A., Bearing Capacity of Shallow Foundations on Unsaturated Soils: Analytical Approach with 3D Numerical Simulations and Experimental Validations, *Int. J. Geomech.*, Vol. 20, No. 3, p. 4019181. (2020).
- [18] Nazariafshar, J., Shafiee, A. and Mehrannia, N., Effect of Construction Method on the Performance of Ordinary and Geotextile-Encased Stone Columns., *Iranian Journal of Science and Technology Transaction of Civil Engineering* vol. 46, issue 6, 2022, pp. 4751–4761.
- [19] Shreya, V., and Peter, E.C.N., A Study of Load Distribution Between Soil and Stone Columns., published in *Ground Improvement Techniques. Proceedings of the Indian Geotechnical Conference Volume 3, 2021.*, Lecture Notes in Civil Engineering, 2023 https://doi.org/10.1007/978-981-19-6727-6_11.
- [20] Gharavi, H., Yazdani, E., Alidoust, P., Shariatmadari, N., Yazdani, F., and Niavol, K. P.,

- Utilization of Shredded Waste Tire as a Substitute for Gravel in Stone Column Groups., *KSCE Journal of Civil Engineering*, vol. 27,2023 pp.198–206. <https://doi.org/10.1007/s12205-022-1731-8>.
- [21] Fattah, M. Y., Shlash, Kais T., and Al-Waily, Maki J., Stress Concentration Ratio of Model Stone Columns in Soft Clays, *Geotechnical Testing Journal*, ASTM, Vol. 34, No. 1, 2011, pp. 61-71, Paper ID GTJ103060 Available online at: www.astm.org.
- [22] Fattah, M. Y., Shlash, K. T., and Al-Waily, M. J., Experimental Evaluation of Stress Concentration Ratio of Model Stone Columns Strengthened by Additives, *International Journal of Physical Modelling in Geotechnics*, ICE, Vol. 13, No. (3), 2013, pp. 79-98, <http://dx.doi.org/10.1680/ijpmg.12.00006>.
- [23] Fahmi, S. K., Kolosov, E.S., and Fattah, M. Y., Behavior of Different Materials for Stone Column Construction, *Journal of Engineering and Applied Sciences*, Vol. 14, No. 4,2019, pp. 1162-1168.
- [24] Bowles, J. E., *Foundation Analysis and Design*, McGraw-Hill Book companies, Inc.1997.
- [25] Sarımurat, S., Işık, N.S., Taşan, H.E., and Firat, S., Numerical investigation of stone columns in liquefiable soils. *Arabian Journal of Geoscience* 15,6:553., 2022, pp.1-14:553, <https://doi.org/10.1007/s12517-022-09804-x>.
- [26] Fattah, M. Y., and Majeed, Q. G., Finite Element Analysis of Geogrid Encased Stone Columns, *Geotechnical and Geological Engineering Journal*, Springer Science+Business Media B.V. 2012, pp. 713–726. DOI 10.1007/s10706-011-9488-8.
- [27] Naik, J. K., Stress-Strain Behavior of Compacted Pond Ash Reinforced with Stone Column, *IOP Conf. Series: Materials Science and Engineering* 970 012032 IOP Publishing, 2020, pp.1-7, doi:10.1088/1757-899X/970/1/012032.
- [28] Fattah, M. Y., Zabar, B. S., and Hassan, H. A., Soil Arching Analysis in Embankments on Soft Clays Reinforced by Stone Columns, *Structural Engineering and Mechanics*, Vol. 56, No. 4, 2015, pp.507-534, DOI: <http://dx.doi.org/10.12989/sem.2015.56.4.507>, Techno press, Korea.
- [29] Shafee, A. and Khoshghalb, A., Augmenting low - order finite element method with partial nodal strain smoothing for flow - deformation analysis of geomechanical problems., *International Journal for Numerical and Analytical Methods in Geomechanics*, vol. 46(17), 2022, pp.3178-3199.

Copyright © Int. J. of GEOMATE All rights reserved, including making copies, unless permission is obtained from the copyright proprietors.
